

INVESTIGATIONS OF A SUPERCONDUCTING BEAM TUBE NIOBIUM CAVITY AT S-BAND

P.Kneisel, O.Stoltz, and J.Halbritter
Kernforschungszentrum und Universität Karlsruhe
Karlsruhe, Germany

Summary

The influence of several surface preparation techniques like electropolishing, chemical edging, anodizing and UVV-heat treatment on both the Q-value and the peak RF fields have been studied in a welded S-band cavity having large beam tubes. Peak magnetic fields up to 650 G at a Q-value of 8×10^{10} in the TE₀₁₁-mode and peak surface electric fields of 25 MV/m at Q = 7×10^9 in the TM₀₁₀-mode have been obtained. Simultaneous measurements of the mean free path in the surface layer of the cavity permit to calculate H_{c1} . The results indicate that H_{c1} is no limitation for the magnetic fields achievable in RF-cavities. This makes type-II-superconductors like Nb₃Sn interesting for practical applications at high frequencies.

I. Introduction

With the preparation of Nb surfaces described in ¹ we have obtained quite regularly surface resistances below $10^{-8} \Omega$ in TM- and TE-modes between 2 and 4 GHz. These residual losses are already small compared to the superconducting part at 1.8°K, where the practical application for high RF fields will take place. ² Therefore we conclude, that residual losses are no longer a problem - in simple GHz cavities - but the breakdown fields obtained are still quite low (<500 G), as yet. These low magnetic thermal breakdown³ fields have been identified in TM-modes as due to electron impact; ¹ especially in multipactor barriers⁴ the enhanced number of electrons easily cause breakdown. The number of fast electrons can be reduced by introducing He-gas (pressure below discharge) into the cold, superconducting cavity. ^{5,6} This "processing with He"⁶ reduces the time to overcome a multipactor barrier and hence the radiation damage, as will be discussed in Part IV. The above mentioned explanation of low H_{crit} due to electron impact works only for TM-modes, but not for the TE₀₁₁-mode, because there is no large electric field to emit electrons. To explain the low H_{crit} of TE-modes one must look for other explanations. Because the H_{crit} of several modes (2-4 GHz) seem to cluster around 400 G a statistical surface roughness cannot be the limitation. If one is looking at volume properties of the superconductor as reasons for an RF breakdown, thermal conductivity, H_{c1} ² or more generally the electron mean free path λ seems important. Because of the observed temperature dependence $H_{crit} \propto H_c(T)$ ^{1,7} the (phonon) thermal conductivity can be omitted as explanation for H_{crit} .³ As discussed in ³ generation and penetration of fluxoids is too slow to cause breakdown for $f \geq 10$ MHz; hence H_{c1} has nothing to do with H_{crit} . About H_{c1} we will show in Part III, that the mean free path λ_s of a surface layer, which is shorter than λ_p of the bulk yields $H_{c1} = 1100$ G at 1.4°K, which is already below the actual observed H_{crit} of 1200⁸-1500 G⁶. Therefore we can conclude, that in RF fields H_{crit} well above H_{c1} can be obtained, which makes, e.g. Nb₃Sn and Nb₃Al

suitable for surface coatings, with which $H_{crit} = H_c = 4000$ G should become possible.

In Part III we report about changes of λ with different surface treatments, but till now nothing about relations between λ and H_{crit} or R_{res} can be said. On the other side we can state about degassing that firing longer than 30h seems not to reduce the bulk mean free path λ_p further. The measured surface mean free path λ_s which describes a mean scattering up to a depth of about 700 Å, seems to be reduced sometimes by (diffuse) surface scattering. In Part IV we report about processing with He, which works even in anodized cavities; for the first time we were able to obtain in the TE₀₁₁-mode a breakdown field of 650 G, which is markedly higher than H_{crit} of TM-modes (≈ 350 G). The residual losses at high field are also quite low, e.g. R_{res} (500 G) = $7.5 \times 10^{-9} \Omega$, corresponding to a Q-value of 10^{11} . It should be mentioned, that these results have been obtained with a beam hole cavity fired at 1900°K in a Nb foil followed by chemical polishing and anodizing.

II. Experimental

Till now all our measurements on residual surface resistance and peak fields were carried out with cylindrical solid niobium cavities of height = diameter = 10.6cm. To be more realistic a electron-beam-welded cavity was constructed as shown in Fig.1, which differed from our earlier cavities in several points: besides beam tubes of 35mm diameter and 110mm length, the cavity was welded out of several niobium parts and has a changed coupling geometry to avoid a heating up of this cavity parts and hence a possible thermal-magnetic breakdown. The beam holes should enable us to carry out chemical and especially electrochemical treatment of the cavity surface¹. In addition only in such a cavity it seems likely to clean the inner surface by an ultrahigh vacuum outgassing³.

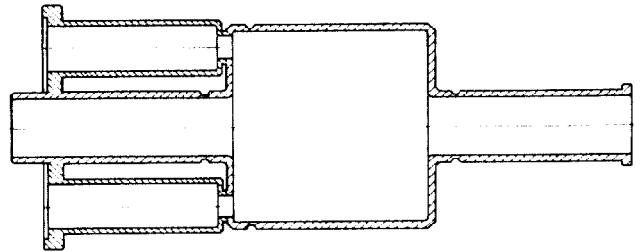


Fig. 1: Schematic drawing of the S-band cavity with beam tubes. The resonator is constructed out of several niobium parts, which have been electron-beam-welded together.

In comparison to our simple cavities the beam tubes have led to a significant increase of the peak electric fields at the cavity surface in the different TM-modes, whereas the magne-

tic fields have been changed only slightly. This enhancement of the peak electric fields caused field limitations due to X-radiation (see Part IV).

Before electron-beam-welding (done by Siemens AG, Erlangen, Germany) the two cavity parts together at the unsymmetric weld the niobium surface was electropolished as described in ¹. Between two polishing cycles the polishing solution was pumped through the beam holes, providing for a faster and more complete solution of the oxide formed during current flow. Besides the measurements of surface resistance and peak-fields - the measuring arrangement and method is described in ¹ - we have measured the mean free path of the bulk-material and of the surface layers, respectively.

The first quantity was measured by the dc-residual resistivity ratio (RRR) using an induction method.⁹ For this case a coil-system (field coil and pick-up coil) was slid over the outer cavity surface and the decay-time of the eddy-currents generated by a pulsed magnetic field were detected at several temperatures.

The measurement of the mean free path of the surface layer consists in the observation of that eigenfrequency change of the cavity with changing temperature in the range $0.6 T_c < T < 0.9 T_c$ which is caused only by the temperature dependence of the penetration depth and not by changes of the geometrical dimensions of the cavity.

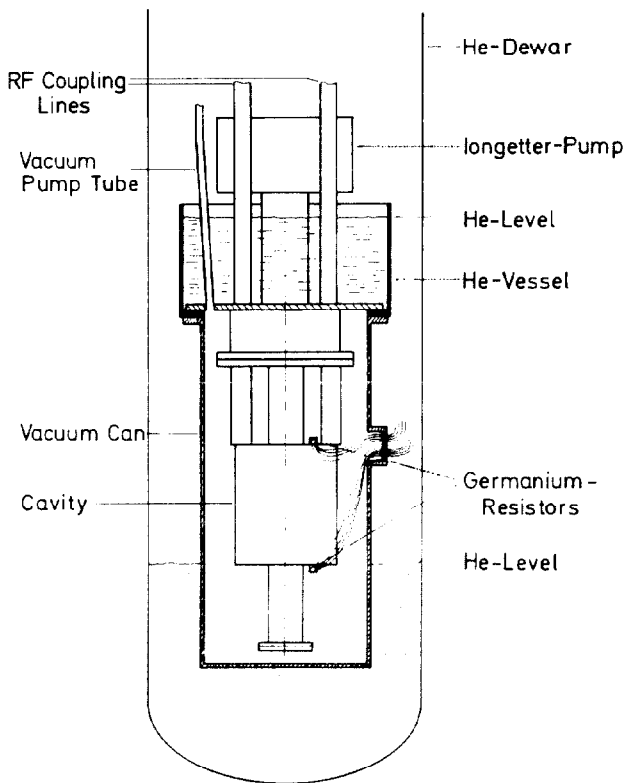


Fig. 2: Schematic drawing of the low temperature part of the experimental set-up used for the measurements of the eigenfrequency change of the cavity above 5°K.

The cavity is surrounded by a vacuum vessel, which not only has to keep off pressure changes in the helium bath but also reduces the temperature gradient along the cavity, which did not exceed 0.1°K in our experiments. He-contact gas of about 10^{-1} Torr provided for a reasonable heat conduction between the helium bath and the cavity. Mistakes in the measurements due to thermal expansion can be excluded below 5°K ($\theta_{D, Nb} > 200^\circ K$).

It should be mentioned that the temperature measurement and the T-gradient over the cavity are no trivial problems and lead to a relatively large uncertainty in the determination of the mean free path.

We report here about a series of measurements, differing from each other by the treatment of the cavity surface as listed below.

Measurement 1: After the last electron-beam-welding was done, the cavity was chemical polished in HNO₃/HF solution at -15°C for 1 minute, rinsed in distilled water and methanol and assembled wet.

Measurement 2: Annealing at 1800°C for 23 h.

Measurement 3: Annealing at 1900°C for 23 h; the cavity was surrounded by a niobium foil of 1mm thickness. Chemical polishing in HNO₃/HF solution at -15°C for 1 min, rinsing in distilled water and methanol and assembling wet.

Measurement 4: Chemical polishing for 1 min in -15°C HNO₃/HF solution. Anodizing in 12.5% NH₄OH-solution at 20V, 0.5 mA/cm² for 15 min. Rinsing in distilled water and methanol and assembling wet.

Results of the measurements are discussed in the following parts.

III. Mean free Paths Measurements

As discussed in ³ the parameters defining H_{crit} are not quite clear. To find relations between H_{crit} and properties of the Nb we have measured the electron mean free path λ . Because the degassing and hence λ depends sensitively on shape of the Nb sample we must measure λ of the RF cavity directly, which we have done by measuring the RRR as described in Part II¹⁵⁻¹⁷. As already observed in Pb²², Ta²³ and Nb¹⁴ the bulk λ_B is longer than λ_S of a surface layer; in addition in transition metals like Ta and Nb λ in the normal conducting state can be different from λ in the superconducting state because of s - d scattering. For the superconducting RF properties we need λ describing the superconducting state near the surface. This mean free path λ_S we have determined by measuring the change of eigenfrequency Δf with temperature (Fig. 3). Because the changes of geometrical dimension by changes of pressure (see Fig.2) and temperature are negligible, Δf is directly related to the penetration depth change $\Delta \lambda(T)$ (G geometry factor)¹⁴

$$\Delta \lambda(T) = \frac{2G}{\mu_0 \omega} \frac{\Delta f(T)}{f_0} = \text{const} \cdot \Delta f(T)$$

and $\Delta f(T) = f(T) - f(T_0)$ is a frequency shift with respect to the value at an arbitrary reference temperature T_0 . In the temperature range $0.6 T_c < T < 0.9 T_c$ the temperature dependence of λ can be approximated by $\Delta \lambda(T) \propto 1/\sqrt{1-t^4}$ with $t = T/T_c$, which is shown by the straight lines in Fig.4, the slopes of

which are roughly proportional to $\sqrt{1+\xi_F/\lambda}^{15,16}$.

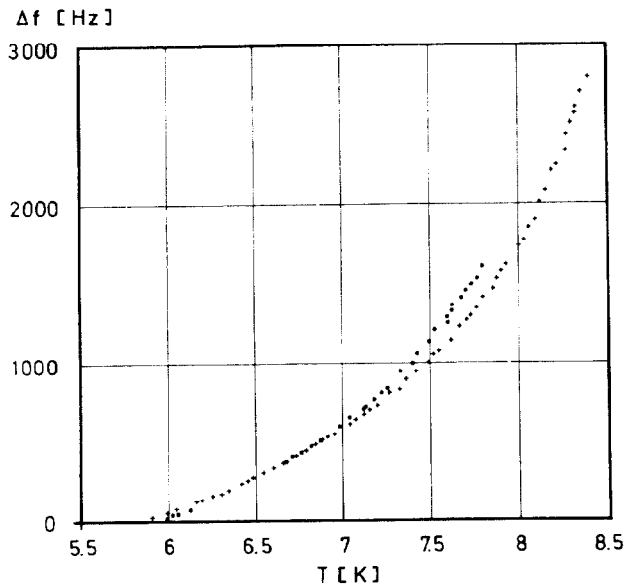


Fig. 3: Typical plot of the increase of the eigenfrequency with temperature for two different mean free paths, measured in the TM_{010} -mode at 2.187 GHz.

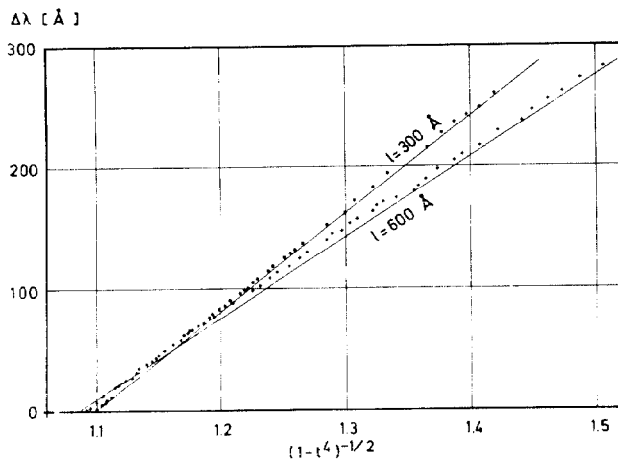


Fig. 4: Penetration depth change corresponding to eigenfrequency change of Fig. 3. The solid lines represent computed dependencies of $\Delta\lambda$ on temperature with electronic parameters given in the text.

If one compares the measured curves with computed ones,¹⁶ which were obtained with the ECS theory for $T_c = 9.25^\circ\text{K}$, $\Delta(0)/kT_c = 1.85$, coherence length $\xi_F = 640 \text{ \AA}$ ($\hat{\xi}_0 = 407 \text{ \AA}$) and London penetration depth 360 \AA ,¹⁷ one can obtain ξ_F/λ (see Fig. 4). This method of using the mean free path dependence of $\lambda(\lambda)$ for the determination of λ is more accurate than the use of the surface resistance $R(\lambda)$, which is for Nb around 3 GHz and $\lambda \approx 300 \text{ \AA}$ nearly independent of λ (Fig. 3).¹⁷

It should be mentioned, that fluxoids should be avoided, because they yield experimentally

an increased slope due to the scattering of the electrons at fluxoids beside the trivial enlargement of the cavity volume by the quasi-normal cores of fluxoids.

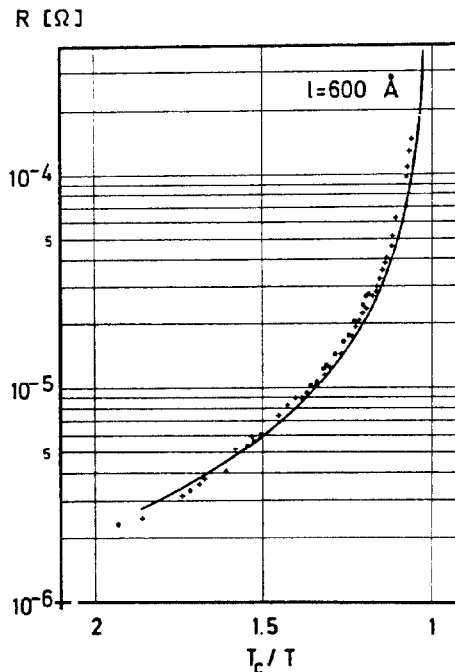


Fig. 5: Surface resistances versus T_c/T for temperatures above 4.2°K corresponding to the $\Delta\lambda$ of Fig. 4. The theoretical solid line for $\lambda = 300 \text{ \AA}$ coincides nearly with the $\lambda = 600 \text{ \AA}$ line.

The resulting mean free paths for the different treatments (Part II) together with the deduced H_{c1} are summarized in Table I.

Table I:

| Treatment | $\lambda_P[\text{Å}]$ | $\lambda_S[\text{Å}]$ | $\kappa_3(1.4^\circ\text{K})_S$ | $H_{c1}(1.4^\circ\text{K})_S$ [Oe] |
|-----------|-----------------------|-----------------------|---------------------------------|---------------------------------------|
| 1 | 600 | 350 | 1.8 | 1170 |
| 2 | 1200 | 550 | 1.55 | 1240 |
| 3 | 1200 | 650 | 1.35 | 1290 |
| 4 | 1200 | 300 | 1.9 | 1110 |

Not heat treated Nb⁸ would yield $H_{c1}(\lambda = 300 \text{ \AA}, 4.2^\circ\text{K}) = 920 \text{ Oe}$.

The κ_3 -values of this Table result from measured H_{c1}/H_c values,¹⁸ yielding $\kappa_3(\lambda = \infty, 1.4^\circ\text{K}) = 0.92$, which then was corrected for finite λ_S according to Gorkov.¹⁹ These corrected $\kappa_3(1.4^\circ\text{K}, \lambda_S)$ then yield²⁰ the H_{c1} values included in the Table.

It should be mentioned that H_{c1} cannot be computed with the aid of the strong temperature dependent κ_1, κ_2 as done in¹¹. The Table shows an improvement in λ_S of Nb by degassing and that λ_P is not enlarged by further firing. It seems that firing in a box consisting of

degassed Nb foil yields the longest λ_S , because the reoxidation during cooling down is hindered; but, as indicated by the scatter of λ_S , $\lambda_S \approx 500 \text{ \AA}$ is changed by surface preparation, which influences the surface scattering of electrons. A relation between λ_S and H_{crit} cannot be deduced, as yet. But it should be mentioned, that the observed H_{crit} of 1200 G⁸ or 1500 G⁸ are already above H_{c1} .

IV. Experimental Results on R_{res} and H_{crit}

The measured $R_{res(min)}$ and H_{crit} values of the new beam hole cavity (Fig.1) after several treatments mentioned in Part II are collected in the following Table II.

Table II:

| | TM ₀₁₀ | TM ₀₁₁ | TM ₀₁₂ | TE ₀₁₁ |
|---------------------------|-------------------|-------------------|-------------------|-------------------|
| f_c [GHz] | 2.187 | 2.637 | 3.636 | 3.743 |
| 1 R_{res} [n Ω] | 2200 | 400 | 910 | 97 |
| 1 H_{crit} [Oe] | - | - | - | 430 |
| 2 R_{res} [n Ω] | 35 | 64 | 67 | 8.7 |
| 2 H_{crit} [Oe] | 160 | 325 | 280 | 270 |
| 3 R_{res} [n Ω] | 23 | 30 | 49 | 7 |
| 3 H_{crit} [Oe] | 330 | 360 | 325 | 510 |
| 4 R_{res} [n Ω] | 25 | 33 | 38 | 6.9 |
| 4 H_{crit} [Oe] | 310 | 340 | 415 | 650 |

This Table shows, that we have successfully adapted the surface preparation methods (see¹) to the beam hole cavity; which is measured like our earlier cavities, in an open vacuum system. The improvement between runs 1 and 2 seem mainly due to an annealing of electron beam welds, which seem bad, because the vacuum in electron beam welders is dirty (C...) and welding yields highly stressed Nb. In addition, only after run 2 our cleaning and rinsing was good enough, so that at this stage (run 1) we used the furnace to evaporate HF, H₂SO₄... Now - after run 3 - we get high Q_0 ($>10^{11}$) and H_{crit} ($>600 \text{ G}$) with polishing or anodizing, without the final heat treatment, which is needed in complicated shaped separator structures.²¹ In our opinion, the needed final heat treatment for complicated large cavities is due to not optimal cleaning of the structures. Astonishingly, in this beam hole cavity we run into a hard multipactor barrier at $H \approx 120 \text{ G}$ which we could not overcome by usual processing in 2 days.⁴ But with He-gas of pressure just below discharge inside the cold cavity we could overcome the barrier in less than 1 h, together with slight improvements of residual losses at high RF field levels (Fig.6), after the He-gas was removed again.

Why helps He processing against electron loading? In the presence of large electron currents, He will be ionized by the electrons. That is, He reduced the energy of electrons and hence the radiation damage (R_{res}) due to the electrons. The ionized He atoms hit the oxidized surface; but because they are slow they are already stopped in a thin surface layer and neutralize there the internal charges of the oxide, which cause the enhanced secondary emission. This mechanism of neutralizing is more gentle than the usual processing with fast electrons, which in addition causes radiation damage. A typical change of $R(R_{pp})$ by processing with He is drawn in Fig.6;

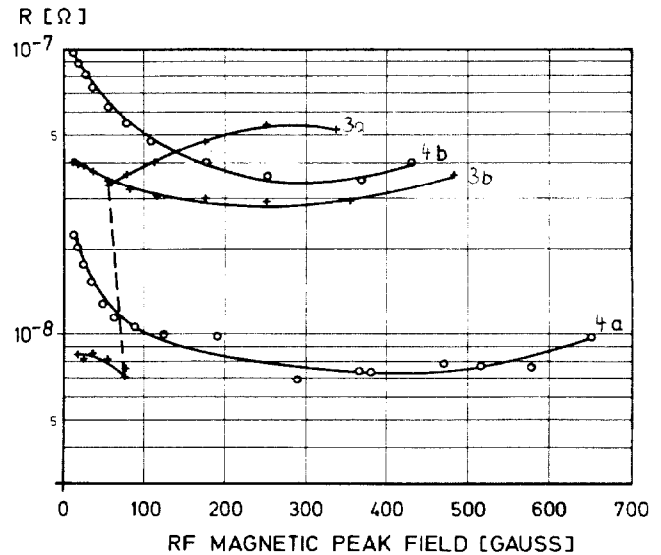


Fig. 6: Amplitude dependence of the surface resistance measured in the TE₀₁₁-mode. Curve 3a was taken during run 3 and shows a typical "switching" at about 80 G. After "processing" with He gas inside the cavity to overcome multipactor barriers in TM-modes the curve 3b was obtained. Curve 4a and 4b belong to run 4 and were achieved initially (a) and after (b) severe X-radiation in the TM₀₁₀ and TM₀₁₁-mode, respectively.

this shows that residual losses are changed by charges in the oxide, which influence interfacial tunneling.²² In addition, the switching¹ observed in run 2 and 3, which seems typical for a chemically grown oxide, disappears after He processing. It is known that an oxide layer enhances electron emission,⁴ e.g. multipactor barriers in anodized cavities could not be overcome,⁵ but with He we were able to overcome the barriers also in an anodized cavity (400 Å Nb₂O₅). In spite of an enhanced γ -radiation in this run we were able to obtain in the TM-modes fields higher than 300 G or 24 MV/m due to the processing; the actual limitation was not magnetic breakdown, but lack of generator power because of the mismatch due to strong electron loading. This strong electron loading in TM-modes caused severe radiation damage, which is shown by the degradation observed in the TE₀₁₁-mode (Fig.6).

V. Conclusion

Our recent measurements have shown that it is possible to transfer surface treatments developed for simple cavities to more complicated shaped ones. A proper cleaning technique after chemical treatments is crucial. Multipactor barriers can be overcome easily with He processing causing less radiation damage than in the case where severe electron loading is present.

In our feeling the high breakdown field of 650 G obtained in the TE₀₁₁-mode is due to the better possibilities of surface preparation and a more favourable shape of our beam hole cavity compared to our simple cavities. An increase of H_{crit} in TM-modes in comparison to a simple, unperturbed cavity could not be

achieved because of field emission loading at 24 MV/m due to a large electric field enhancement. Measurements of the mean free path in the surface layer of our cavities indicate that H_{c1} seems to be no limitation for the magnetic fields H_{crit} obtainable in RF-cavities. This result makes the use of type II superconductors with high T_c like Nb_3Sn , Nb_3Al suitable for the application in RF superconductivity.

Acknowledgement

The authors would like to thank P.E.Wilson for computing the fields in the beam tube cavity.

References

- ¹P.Kneisel, thesis (Universität Karlsruhe, 1972); P.Kneisel, O.Stoltz, J.Halbritter; Proc.1972 Appl.Superconductivity Conf., Annapolis, 1972 (IEEE Pub.No.72CH0682-5-TAESC), p.657
- ²J.P.Turneure, *ibid*, p.621
- ³J.Halbritter, *ibid*, p.662
- ⁴J.Halbritter, Part.Acc.3, 163 (1972); P.Kneisel, O.Stoltz, J.Halbritter; J.Appl.Phys.44, April (1973)
- ⁵M.S.McAshan, H.A.Schwettman, L.Suelzle, J.P.Turneure, HEPL-report-665 (Stanford University, 1972)
- ⁶H.Diepers et al., this conference
- ⁷C.Lyneis, thesis (Stanford University,1973)
- ⁸P.Piosczyk et al., this conference
- ⁹C.P.Bean, R.W.DeBlois, L.B.Nesbitt, JAP 30, 1976 (1959); A.F.Clark, V.A.Deason, J.G.Hust R.L.Powell, NBS-Publication 260-39 (1972)
- ¹⁰J.Hasse, C.Lyneis; private communication
- ¹¹E.L.Garwin, M.Rabinowitz; Appl.Phys.Lett.20, 154 (1972)
- ¹²J.Lachmann, J.Hasse, Z.Physik 258, 136 (1973)
- ¹³M.Strongin et al., Ref.2, p. 667
- ¹⁴J.Halbritter, J.Appl.Phys.41, 4581 (1970)
- ¹⁵J.Halbritter, Z.Physik 243, 201 (1971)
- ¹⁶J.Halbritter, Externer Bericht 3/70-6 (KFZ, Karlsruhe, 1970)
- ¹⁷J.Halbritter, Z.Physik 238, 466 (1970)
- ¹⁸J.Auer, H.Ullmaier, Phys.Rev.E7, 136 (1973) and private communication
- ¹⁹L.P.Gorkov, JETP 10, 998 (1960)
- ²⁰J.L.Harden, V.Arp, Cryogenics 3,105 (1963)
- ²¹W.Bauer et al., this conference
- ²²J.Halbritter, Phys.Lett.(1973)